Heliyon 10 (2024) e38957

Contents lists available at ScienceDirect

Heliyon

journal homepage: www.cell.com/heliyon

Research article

Typical NF2 and LTZR1 mutations are retained in an immortalized human schwann cell model of schwannomatosis

Valentina Melfi [a,1], Tasnim Mohamed [a,1], Alessandra Colciago [a], Alessandra Fasciani [b], Raffaele De Francesco [a,c], Daniela Bettio [d], Cristina Cerqua [d], Francesca Boaretto [d], Elisabetta Basso [e], Stefano Ferraresi [e], Marco Montini [f], Marica Eoli [g], Laura Papi [f], Eva Trevisson [d,**], Valerio Magnaghi [a,*]

[a] *Dept. of Pharmacological and Biomolecular Science "R. Paoletti" Università degli Studi di Milano, Italy*
[b] *Human Technopole, Milan, Italy*
[c] *INGM, Istituto Nazionale Genetica Molecolare "Romeo ed Enrica Invernizzi", Milan, Italy*
[d] *Clinical Genetics Unit, Dept. of Women's and Children's Health, University of Padova, Italy*
[e] *Dept. of Neurosurgery, Ospedale Santa Maria della Misericordia, Rovigo, Italy*
[f] *Dept. of Experimental and Clinical, Medical Genetics Unit, Biomedical Sciences "Mario Serio," University of Florence, Florence, Italy*
[g] *Neuro Oncology Unit, Fondazione IRCCS Istituto Neurologico Carlo Besta, Milan, Italy*

A B S T R A C T

Human SCs play a primary role in SWN, a rare genetic disorder in which patients develop multiple schwannomas. So that, their isolation and immortalization could represent an irreplaceable tool to investigate the disease etiopathology. Although few clones of tumoural SCs have been obtained, unfortunately they present genetic, morphological and biological characteristics that do not fully represent the original cells. Herein we isolated, characterized and immortalized primary SCs from human schwannomas. Our immortalized human SCs present typical *NF2* and *LTZR1* genetic mutations of SWN and retain original phenotype characteristics, representing a valuable tool for further genetic, functional and biomolecular *in vitro* studies.

1. Introduction

Schwannomatosis (SWN) is a rare genetic disorder, with a prevalence of 1/40000–1/70000 births [1]. SWN and neurofibromatosis type 2 are clinically and genetically distinct entities, although they share many common features. Diagnostic criteria for these two conditions have been recently updated by integrating the recent molecular and clinical advances and it was established to use "schwannomatosis" classified according to the causative gene, while abandoning the term "neurofibromatosis" [2]. Nevertheless, SWN patients might still be misdiagnosed with neurofibromatosis type 2 or other nerve tumour disorders, thus its prevalence seems to be underestimated.

Patients with classical SWN develop multiple intracranial, spinal or peripheral schwannomas, whereas the vestibular nerve is generally unaffected. The occurrence of bilateral vestibular schwannoma, instead, is pathognomonic of the neurofibromatosis type 2 [1]. However, unilateral vestibular schwannoma is not specific since it has been reported in patients affected by SWN [3,4], and even

* Corresponding author.
** Corresponding author.
E-mail addresses: eva.trevisson@unipd.it (E. Trevisson), valerio.magnaghi@unimi.it (V. Magnaghi).
[1] Valentina Melfi and Tasnim Mohamed are co-first since participated equally to this paper.

https://doi.org/10.1016/j.heliyon.2024.e38957
Received 19 June 2024; Received in revised form 26 September 2024; Accepted 3 October 2024
Available online 4 October 2024

other clinical features may overlap between pathologies. In fact, mosaic neurofibromatosis type 2 may present with multiple schwannomas and/or meningiomas in the absence of bilateral or unilateral vestibular schwannomas [2,5]. Nevertheless, there are reports of single or multiple meningiomas in patients with a clinical diagnosis of SWN [6,7] and these tumours have been reported also in patients with familial SWN, presenting both schwannomas and meningiomas [8] or meningiomas alone [9]. The consequence of this clinical overlap is that SWN patients might be misdiagnosed as having neurofibromatosis type 2 [4] and that a proper approach requires comprehensive molecular genetic testing. The dominant clinical symptom of SWN is chronic nagging pain, which usually but not always develops when a schwannoma enlarges, compresses nerves or adjacent tissue, and its occurrence in association with the tumour increases the probability of SWN [10].

Unlike neurofibromatosis type 2, which is caused by germline or mosaic pathogenic variants in the *NF2* gene (coding for the protein merlin) on chromosome 22q11.2, SWN is genetically heterogeneous. Indeed, tumours from SWN patients frequently harbour the classic truncating mutations of the *NF2* gene and loss of heterozygosity of the surrounding region of chromosome 22, but no heterozygous *NF2* pathogenic alterations are detected in normal tissues. Exploration of multiple tumours from the same patient showed somatic changes in *NF2*. However, each tumour harbours a unique pathogenic variant, not present in other tumours from the same patient. This scenario implied that the primary event in the tumours reclines out of the *NF2* coding region, suggesting the involvement of locus close to this gene in schwannomas pathogenesis. Additionally, mutations in two genes have been associated with SWN: *SMARCB1* [11] and *LZTR1* [12,13]. *SMARCB1* maps on chromosome 22q22.1 and encodes SNF5 or INI1, a subunit of the SWI/SNF (BAF) ATP-dependent chromatin-remodelling complex, which exerts crucial functions and is highly conserved throughout evolution [14]. *LZTR1*, which is closely linked to *NF2* and *SMARCB1* on chromosome 22, encodes for a protein belonging to a functional superfamily of BTB/POZ (broad complex, tramtrack, and bric-a-brac/poxvirus and zinc finger) proteins. The BTB-containing proteins regulate some basal cellular processes, such as chromatin control or cell cycle regulation [13]. However, beyond biallelic mutations of *SMARCB1* or *LZTR1* often detected in tumours of SWN patients, in general, *NF2* is also somatically inactivated by schwannoma-specific mutations, with 22q loss that include the wild copies of *NF2* and *SMARCB1/LZTR1*. Based on these findings, a 4-hit/3-step mechanism was proposed as a model for tumorigenesis [15]. This mechanism evokes the former studies of Sestini [16] and Paganini [12] demonstrating that a germinal mutation of *SMARCB1* or *LTZR1* is generally followed by the somatic mutation of *NF2* on the same allele, and by the loss of the wild-type allele of both *SMARCB1 or LTZR1* and *NF2* on chromosome 22. Overall, the causative genes involved remain unknown in a significant portion of SWN patients and this may depend on the presence of mosaic *NF2* or the presence of mutations in other genes, hitherto unidentified.

Hence, genetic heterogeneity and clinical overlap make SWN diagnosis complicated, so that more accurate diagnostic tools and tests are needed, including the analysis of both blood and tumours. In this regard, the recognition of other genes and/or pathogenic mechanisms responsible of SWN was limited by the paucity of reliable *in vitro* cellular models of human schwannomas. The principal aim of our study was the isolation, purification and characterization of hSCs derived from human schwannomas. Furthermore, since SCs from schwannoma are benign cells proliferating only few passages before senescence, and are difficult to grow in culture, we developed an immortalized primary cell line. Our hSCs present typical genetic mutations of SWN, and retain original phenotype features following immortalization and *in vitro* passaging, representing a reliable tool for further *in vitro* studies.

2. Methods

2.1. Tissue collection and ethical issues

Some human schwannoma tumours were gathered from a surgical case from Hospital “Santa Maria della Misericordia” (Rovigo, Italy). All procedures were approved by the Ethical Committee of UNIMI (PRIN-2017BJJ5EE; Ethical Approval 95/2020). The peripheral tumour specimens were collected in Hanks’ Balanced Salt Solution (HBSS, R&D Systems) for delivery, under short-term maintenance of cells in the absence of O_2. Material was obtained following written informed consent of patient from the Hospital “Santa Maria della Misericordia” (Rovigo, Italy).

2.2. Primary cell culture preparation

Tissue around the schwannoma specimens was pulled out, and the tumoural tissue treated by enzymatic digestion for 30 min with collagenase (Worthington 0.125 mg/mL) and dispase (Gibco 0.50 mg/mL). Cell suspension was then filtered, centrifuged at 1200 rpm, and the pellet suspended in medium [DMEM (Serotec), FBS 10 % (Thermo Fisher Scientific), 2 μM forskolin (Merk), 20 ng/ml glial growth factor-GGF (R&D System)]. The cells were plated on poly-l-lysine (Merk) coated petri dishes until 80 % confluence was reached. Cells were then split or frozen [in DMEM +20 % FBS+ 10 % DMSO (Merk)] for further use. Cell purification was done by MACS MicroBeads immunomagnetic selection method (Myltenyi Biotec), based on SCs specific surface expression of p75 neurotrophin receptor, p75NTR (CD271). Mixed cells were incubated with anti-CD271 (1:100; Miltenyi Biotec, #130-091-885), and then purified through 2-column passages. The eluted SCs were ready for further cultivation *in vitro* in DMEM, FBS 10 %, 2 μM forskolin, 20 ng/ml GGF.

2.3. Cell immortalization

The Ef1a_Large T-antigen_Ires_Puro, a lentiviral plasmid expressing SV40 large T antigen (LT) (Addgene; #18922) was used to immortalize the hSCs according to manufacturer’s instructions. Lentiviral vectors were produced by transient transfection into

HEK293 cells (System Bioscience) seeded in Iscove modified Dulbecco medium. HEK293 cells were seeded at 5×10^3 cells/cm^2 in DMEM medium with supplements. The next day, cells were transfected using the 2.5 M $CaCl_2$ method with packaging vectors pREV (Addgene, #12253), pMDL (Addgene #12251), pVSVG, and the transfer vector in a 1:1.44:2:5.12 ratio. After 16 h, the medium was changed with ISCOVE medium with supplements. Following 30 h, the medium was harvested, filtered, centrifuged 2 h at 20,000 rpm, and the viral vector pellet was suspended in PBS, then stored at −80 °C.

2.4. Immunofluorescence (IFL)

SCs morphology was tested by IFL and CLSM (confocal laser scanner microscopy). Cells plated on coverslips were fixed in 4 % paraformaldehyde (Merk Sigma-Aldrich). Aspecific binding sites were blocked with 0.25 % BSA (Bovine serum albumin - Sigma Aldrich); cells were then incubated overnight at 4 °C in PBS, 0,1 % Triton X-100 with the specific primary antibodies: anti-S100 (1:150; Dako Agilent Technologies), detecting cells of SCs origin; anti-Thy-1 (1:200, Abcam), detecting fibroblasts. The following day, slides were rinsed in PBS and incubated with secondary antibodies: Alexa-Fluor 488 and/or Alexa-Fluor 568 (Thermo Fisher Scientific); slides were then washed, and mounted using Vectashield™ with DAPI. Negative controls lacked primary antibodies. CLSM was done by Zeiss and by Zen software analysis (Zeiss). Cell count analysis of S100+ cells was performed matching purified vs. residual cultures from 6 specimens; petri dishes (purified vs. residual) from each specimen was counted under 40X magnification, using ImageJ (version 1.53c NIH) for image processing and quantification. At least 5 diagonal fields per petri (covering more than 40% of total surface) were counted.

2.5. Flow cytometry

Cells were collected and suspended in FxCycle PI/RNAse staining solution (Invitrogen, Thermo Fisher Scientific), for 30 min in dark. Following incubation with the specific antibodies anti-CD271 (1:100; Miltenyi Biotec, #130-113-410) and anti-CD45 (1:100; Miltenyi Biotec, #130-110-632) respectively, fluorescence was tested with Novocyte 3000 (ACEA Biosciences). Results are expressed as fluorescent intensity *vs.* number of events; for each analysis 10^4 event were counted. The NovoExpress software was used for analysis.

2.6. Western blot

Cells were lysed with RIPA buffer plus protease inhibitors (all by Merk Life Science), then centrifuged 12.500 rpm for 15 min at 4 °C; the supernatant proteins were quantified by BCA kit (Thermo Fisher). Equal amounts of each sample (10 μg of proteins) were resolved by SDS-PAGE electrophoresis and transferred to nitrocellulose membrane (GE Healthcare). Following blocking, the membranes were incubated overnight with the primary antibodies: mouse anti-SV40 (1:1000; Thermo Fischer) and anti-GAPDH (1:2000; Merk Life Science); then, the membranes were incubated with HRP-conjugated anti-mouse secondary antibody and revealed with chemiluminescence (Cyanagen Ultra). GAPDH levels were used as control. Analysis was done by Chemidoc MP Imaging System (Bio Rad Laboratories).

2.7. NGS analysis

Genomic DNA was obtained from immortalized cells by using MagPurix Blood DNA Extraction Kit (Resnova). The coding sequences of genes associated with SPS (*LZTR1*, *NF2* and *SMARCB1*) were captured using the SureSelect Enrichment system (SureSelect QXT); indexed DNA fragments libraries were obtained in accordance to the manufacturer's protocol (v. D.5) and sequenced on a MiniSeq Dx instrument (Illumina), with 150 bp paired-end sequencing. Bioinformatic analyses for NGS experiments were done using the SureCall software v3.0.2.1 (Agilent Technologies). The Genbank accession numbers for human *LZTR1*, *NF2*, *SMARCB1* are NM_006767.4, NM_000268.4 and NM_003073.5, respectively. Copy number analysis was performed using the SureCall software. Variants were classified according to the ACMG criteria [17].

2.8. Cytogenetic and interphasic fluorescence in situ (iFISH) analyses

The immortalized hSCs were cultivated for 48–72 h in RPMI-1640 medium plus 10 % FBS, before the complete confluence, then stopped with Colcemid (10 μg/ml) for the last 4/5 h of incubation. Following harvesting, the cells were then centrifuged for 10 min and the supernatant discarded. Five ml of KCl hypotonic solution (0.075 M) was added to the cells, that were incubated for 10 min, then pelletted and fixed 10 min with 5 ml of Carnoy's fixative, and finally centrifuged. This step repeated 2–3 times until the pellet was white. The cell suspension on dropped on a wet slide, and the slides incubated at 37 °C for 15–20 min. QFQ-banding was done using Quinacrine Mustard. Cytogenetic analysis was performed on Q-banded metaphases at a resolution of 300 bands using the Zeiss M2 Axioplan 2 imaging microscope. Chromosomal anomalies were reported accordingly to the most updated International System for Human Cytogenetic Nomenclature [18]. iFISH analysis was performed, following standard procedures, in order to verify chromosome 22 monosomy in the nuclei, avoiding misinterpretation caused by possible chromosome 22 random loss in the metaphases due to technical artefact. A specific probe for locus 22q11.2, LSI TUPLE1 labelled in orange, was used with a control locus, LSI ARSA, mapped in 22q13.3 and labelled in green (Vysis-Abbott).

2.9. Statistical and bioinformatic analysis of transcriptome

Statistic was done by GraphPad Prism 8.00, using the following tests: parametric *t*-test and/or two-way ANOVA with Krystal-Wellis post-test.

3. Results

3.1. Isolation and assessment of primary hSCs from schwannoma

We obtained encapsulated schwannoma specimens, (Fig. 1A), from a patient presenting a well-stated clinical case of SWN. The peripheral tumours caused dysesthesia, pain and the patient presented Tinel's sign. If compared to non-encapsulated tumours, the specimens used are more suitable for the cell preparation. In general, following tumour digestion and culturing, primary hSCs cultures were separated by positive selection with QuadroMACS™, based on the expression of the p75NTR (CD271) on their cell membrane.

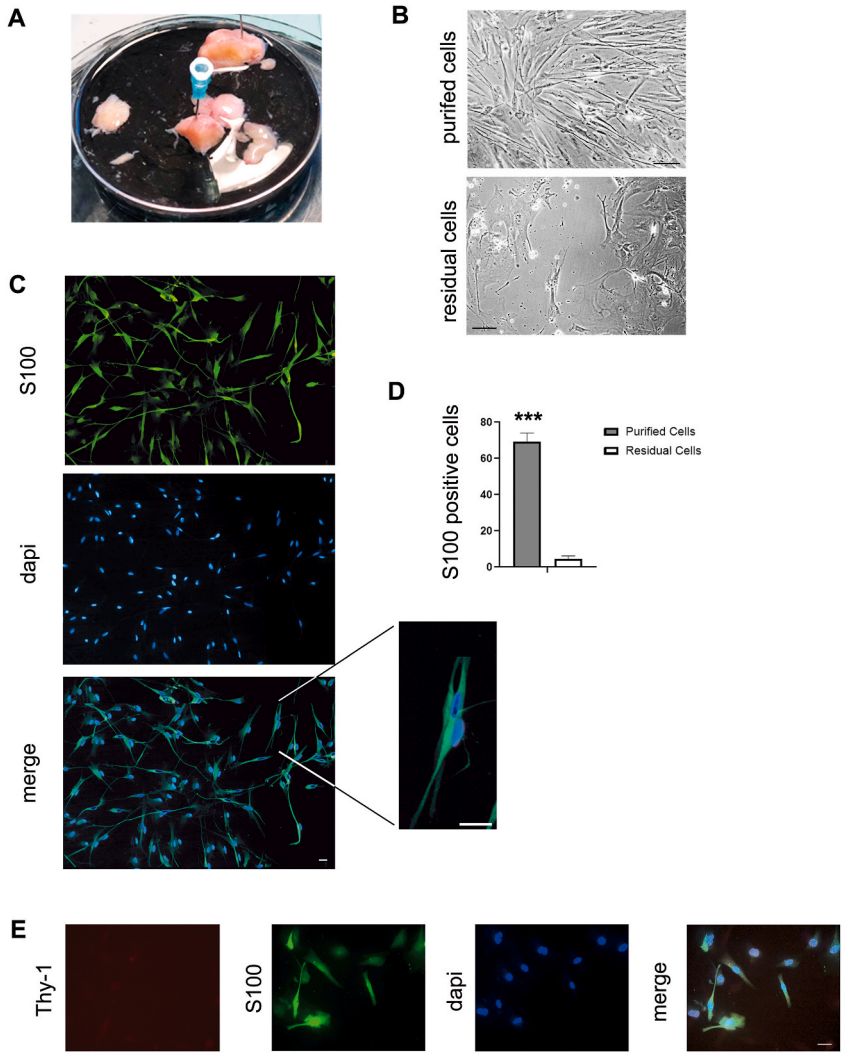

Fig. 1. Assessment of primary hSCs from schwannoma. A) Representative image of different encapsulated schwannomas, that underwent cell isolation procedures; **B**) Image of primary hSCs in culture following positive p75 receptor immunoselection. The fraction enriched in purified cells presented the typical spindle-shape morphology, that was not evidenced in the residual cells; scale bar 10 μm; **C**) IFL images showing the immunopositivity for the typical SCs marker S100 (green). Dapi stained the nuclei (blue); merge images were double-stained. See also a magnification of some cells, showing the fusiform morphology, typical of differentiated SCs. Scale bar 10 μm. **D)** Quantitative morphometric analysis of S100+ cells in purified *vs*. residual hSCs cultures. Around 70 % of S100+ cells (69.05 ± 4.93 %; n = 6; ***p < 0.001 *vs.* residual) were found in purified SCs culture, while in the residual cell the percentage was low (4.46 ± 1.66 %; n = 6). **E)** Images of IFL analysis for the fibroblast marker Thy-1 (in red). SCs labelled for S100 (in green). Dapi stained the nuclei (blue); merge images were triple-stained. Scale bar 10 μm. (For interpretation of the references to colour in this figure legend, the reader is referred to the Web version of this article.)

After the first week in culture, the fraction of purified cells was enriched with SCs, presenting the typical spindle-shape morphology; residual cells, instead, showed a morphology completely different from typical SCs (Fig. 1B). Purified and residual SCs were assessed by using a primary anti-S100 antibody, a characteristic marker of glial cells such as the SCs. As showed in Fig. 1C, S100+ cells exhibited fusiform morphology, typical of differentiated SCs, giving further confirmation of the factual enrichment of the SCs culture following purification. Immunolabelling quantification showed a significant quantity of S100+ cells (69.05 ± 4.93 %; n = 6; ***$p < 0.001$) in the purified SCs culture *vs.* the residual cells, in which the percentage of S100+ cells was extremely low (Fig. 1D), further

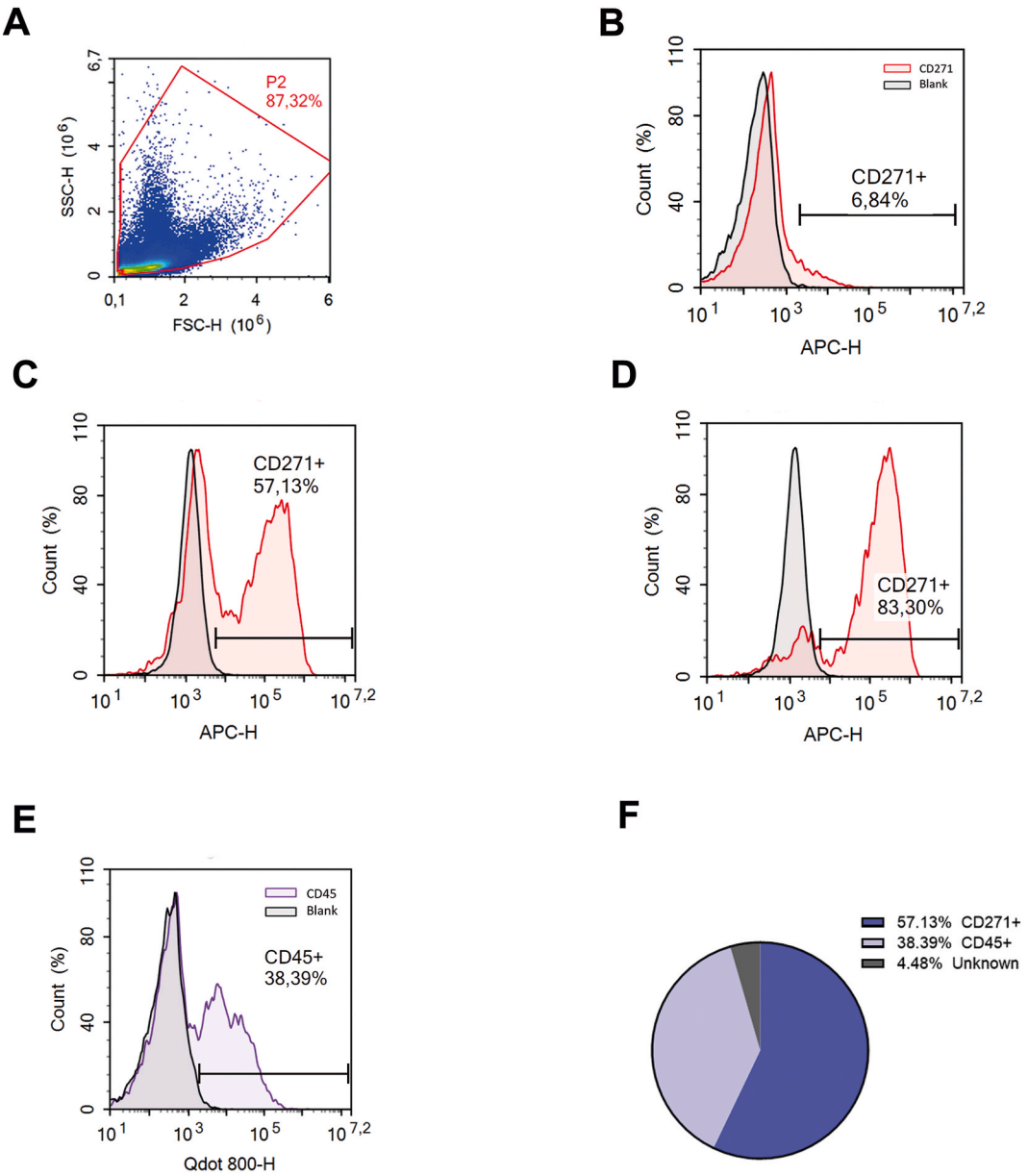

Fig. 2. Flow cytometry characterization of hSCs from schwannoma. A) Representative cytofluorimetric diagram dot-plot forward scatter (FSC-H) *vs.* side scatter (SSC-H; 106) of pre-purified cell population obtained from primary cell preparation. The P2 area (highlighted in red) represents the total cell population analysed (87.32 %), from which cell debris has been excluded; **B)** Representative cytofluorimetric dot-histogram of CD271+ cells (red peak), showing that just after post-tumour digestion only the 6.84 % of cells were immunopositive; **C)** The CD271+ cells (red peak) rose to 57.13 % one week after culturing; **D)** Then following purification the CD271+ cells (red peak) increased to 83.30 %; **E)** Before purification, the 38.39 % of the mixed culture was composed by $CD45^{+}$ cells (violet peak). In all dot-histograms (**B, C, D, E**), results are expressed as fluorescent intensity *vs.* number of events; for each analysis 104 event were counted; APC-H, allophycocyanine fluorescent label; Qdot 800-H, fluorescent label (Thermo Fischer); **F)** Chart representing the percentage of cells of different origin in the mixed culture, before purification: 57.13 % CD271+ cells; 38.39 % CD45+ cells; 4.48 % unknown cells. (For interpretation of the references to colour in this figure legend, the reader is referred to the Web version of this article.)

confirming the enrichment (around 70 %) of SCs in our primary culture. As expected, fibroblast contamination of purified hSCs was confirmed by the lack of Thy-1 (specific fibroblast marker) immunostaining (Fig. 1E).

3.2. Flow cytometry characterization

Pre-purified, purified and residual hSCs were assessed by flow cytometry. The P2 area highlighted in red in Fig. 2A represents the pre-purified cell population analysed (87.32 %), with the exclusion of cell debris. The data obtained indicated that only the 6.84 % of CD271+ cells were present in the post-tumour digestion (Fig. 2B). One week after growing in culture, the mixed cell showed about 57.13 % of CD271+ cells (Fig. 2C), then following purification the percentage of CD271+ hSCs rose to 83.30 % (Fig. 2D). Mixed cell culture, before purification, showed 38.39 % of CD45+ cells (marker of leucocytes), indicating the presence of immune-related cells in the mixed cell culture, directly coming from the tumour mass (Fig. 2E). Overall, the diagram in Fig. 2F summarizes the percentage of different cells in the mixed culture, after one week *in vitro* but before purification: 57.13 % CD271+ cells; 38.39 % CD45+ cells; 4.48 % unidentified cells.

3.3. Immortalization and assessment of hSCs from schwannoma

Since purified hSCs from schwannoma tumours are difficult to grow in culture, we developed an immortalized primary cell line. Thus, hSCs were transduced with the lenti-LTAg-SV40 at MOI-3. The hSCs proved able to acquire the lentiviral vector, indeed they expressed the relative SV40 protein levels (94 kDa; see Fig. 3A) at different passages *in vitro*. Immortalized hSCs maintained the

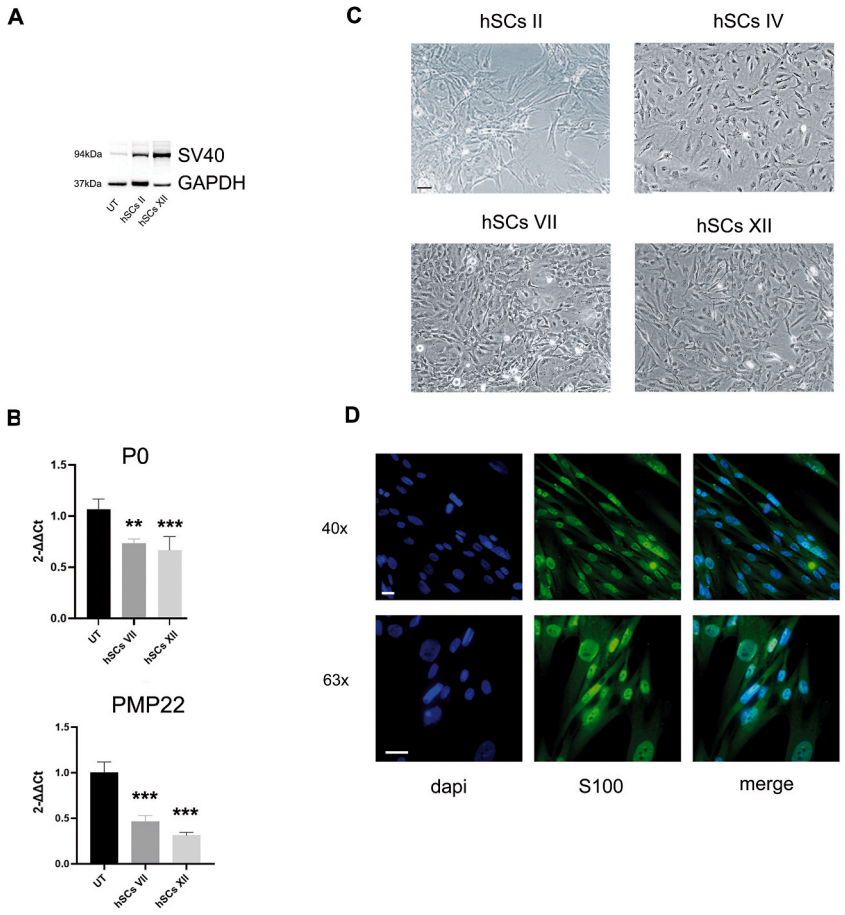

Fig. 3. Immortalization of hSCs from schwannoma. A) Representative immunoblot of the SV40 protein (94 kDa) in hSCs following immortalization, at different cell passages (II to XII). The housekeeping was GAPDH; control SCs (UT) were not transformed with SV40; **B**) Expression levels of the typical SCs markers P0 and PMP22 were significantly expressed [**$p < 0.01$; ***$p < 0.001$ vs. control untransfected SCs (UT)] at different cell passages *in vitro* (VI, VII, XII)); Values are means ± s.e.m. ($n = 6$). All statistical analysis were done with one-way ANOVA and Dunnett's post-hoc test; **C**) Images of immortalized hSCs at progressive culturing passages (II to XII passage); cells retained the typical spindle-shape morphology; scale bar 10 μm; **D**) IFL images showing the immunopositivity for the S100 (in green), until XII passage following immortalization. Nuclei were stained with dapi (in blue); merge images were double-stained. Scale bar 10 μm. (For interpretation of the references to colour in this figure legend, the reader is referred to the Web version of this article.)

expression of typical SCs genes, such as the myelin protein zero (i.e. P0) and the peripheral myelin protein of 22 kDa (i.e. PMP22), for more than XII passages *in vitro* (Fig. 3B). Moreover, immortalized hSCs showed the typical spindle-shaped morphology and high proliferation at different *in vitro* passages, until XII passage (Fig. 3C); this feature was corroborated by the IFL analysis of immortalized hSC for the specific marker S100, further confirming the SCs phenotype at later passages, such as the XII *in vitro* (Fig. 3D). Furthermore, NGS sequencing of DNA from schwannoma-derived immortalized hSCs cells at high passage (XII passage *in vitro*) detected two loss of function variants in genes associated to the SWN predisposition syndrome (SPS), and in agreement with the diagnosis of schwannoma: a single nucleotide duplication in exon 1 of *LZTR1* [with variant allele frequency (VAF) of 64 %] and a deletion affecting the splicing acceptor site of exon 5 in *NF2* (VAF 32 %) (Table 1). The first variant, which was previously detected in *LZTR*-related SPS patients [13] and in autosomal recessive Noonan syndrome [19], is predicted to insert a premature stop at codon 128. It is reported in the gnomAD v4.1.0 database with an allele frequency of 0.006 %, in agreement with the well-known lack of penetrance of *LZTR1* variants [20]. The 26-nucleotide deletion at the 3′ splice junction of *NF2* was never reported either in the scientific literature or in population or mutation databases (absent in gnomAD v4.1.0, Leiden Open Variation Database - LOVD, ClinVar and COSMIC) and is predicted to affect transcript maturation by disrupting the acceptor site (Splice AI and Human Splicing Finder). According to ACMG criteria, the *LZTR1* change and the *NF2* deletion were classified as class 5 and class 4, respectively (Table 1). Copy number analysis (CNV) of NGS data using the SureCall software suggests the presence of 22q loss, predicting a deletion involving the *LZTR1*, *SMARCB1* and *NF2* genes. The molecular signature of immortalized hSCs cells is compatible with the 4 hits/3 step model previously proven for the genesis of schwannomas [12,13,21].

3.4. Cytogenetic characterization of immortalized hSCs from schwannoma

Cytogenetic analysis detected two equally represented cell lines. One exhibits a range of 40–45 chromosomes (hypodiploid range according to ISCN) and the presence of many telomeric associations (TAS) between chromosome ends, so that they appear to be a single chromosome but are counted as two. Loss of chromosome 22 was observed in all the 20 metaphases analysed, probably derived from a parental cell line 45,XY,-22, along with non-specific chromosome random loss (Fig. 4A). The other cell line showed 82 to 88 chromosomes, a hypotetraploid range, and multiple TAS. All these cells retain two copies of chromosome 22, as expected from a starting cell line with 45 chromosomes and 22 loss. The structural rearrangements found in our cell lines are predominantly TAS, that along with tetraploidy, are a well-known phenomenon occurring in tumour cells [22,23]. In order to confirm chromosome 22 monosomy in the nuclei, avoiding misinterpretation caused by possible chromosome 22 random loss in the metaphases due to technical artefact, iFISH was performed. The analysis detected only one orange and one green signal in 100 nuclei analysed, confirming the loss of one chromosome 22 in the cell line with 40–45 chromosomes (Fig. 4B). In other 100 nuclei scored, two signals for each probe were observed, demonstrating the duplication of chromosome 22 in the hypotetraploid cells harbouring a range of 82–88 chromosomes.

4. Discussion

Here we obtained a line of immortalized hSCs, highly purified from a human schwannoma, bearing histological and molecular characteristics of SWN, also longitudinally for over 12 passages *in vitro*.

SPS is an adult-onset syndromic condition distinguished by multiple schwannomas development. Namely, SPS is a general term to define the pathogenic predisposition to develop schwannomas, whereas the genetic modification of peculiar causative genes (i.e. *NF2, SMARCB1* and *LZTR1*) may lid to classification of specific forms of SWN: NF2-, SMARCB1- and LTZR1-related SWN [24]. In any case, schwannoma tumours arise from the SCs of spinal and/or peripheral nerves. Homozygous inactivation of the SPS-associated genes *SMARCB1* and *LZTR1* is embryonically lethal [25,26]; hence, a conditional mouse model of SPS was generated by ablating *SMARCB1* and *NF2* in SC lineage in specific developmental stages, further confirming the requirement of both genes in schwannoma development [26]. The availability of preclinical models is therefore crucial to develop efficient treatments. However, developing animal models is time consuming and may show only part of the clinical manifestations, considering the wide spectrum of mutations in SPS-associated genes and the limited knowledge of genotype-phenotype correlations. In addition, models for drug discoveries should be based on mutations found in patients and therefore clinical trials might benefit of different approaches. Remarkably, the availability of patient-derived cell models in SPS would be helpful for drug screening in order to study novel personalized drugs able to counteract tumour growth and the excruciating associated pain.

The first attempts of generating cellular models date back to an early work by Hung and collaborators [27], which obtained a primary cultures of schwannoma of vestibular origin from a patient affected by neurofibromatosis type 2. These cells were characterized and isolated, albeit incompletely, through immunocytochemistry, RT-PCR and non-isotopic RNAse Cleavage (NIRCA) assays,

Table 1
Identified gene variants in immortalized hSCs.

	Variant	Effect on protein	VAF	ACMG criteria	Reported
LZTR1	NM_006767.4:c.27dup	p.(Gln10Alafs*2 4)	64 %	Class 5 pathogenic (PVS1vs, PM2sup, PP5s)	ClinVar 24362817 32623905
NF2	NM_000268.4:c.448-21_452del	p.(?)	32 %	Class 4 likely pathogenic (PVS1s, PM2sup	–

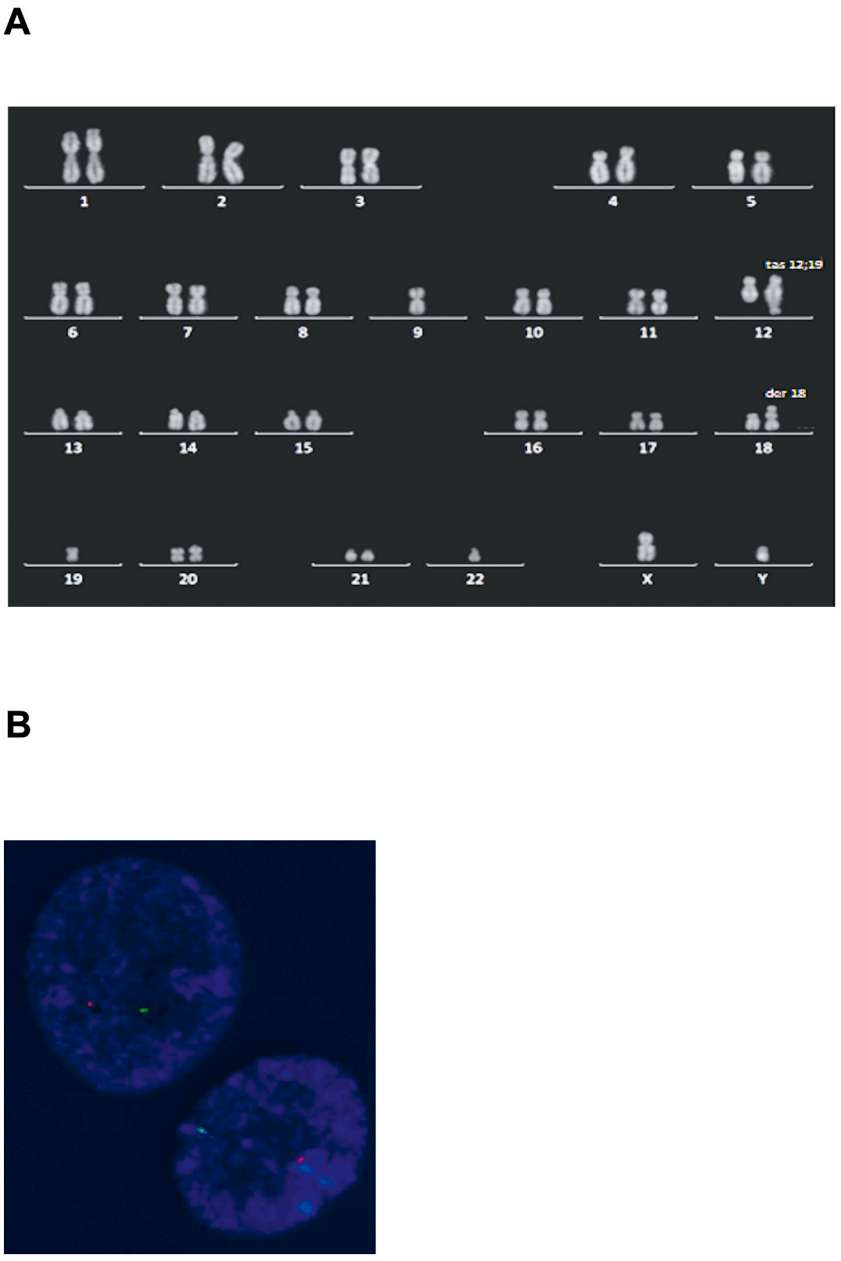

Fig. 4. Cytogenetic characterization of immortalized hSCs from schwannoma. A) Representative image of a Q-banded metaphase showing monosomy of chromosome 22 and two TAS: the first between the chromosome 12 long arm and the chromosome 19 short arm; the second between the chromosome 9 short arm and the chromosome 18 long arm**; B**) iFISH of two nuclei demonstrating the presence of only one green (*ARSA* control locus) and one orange signal (LSI TUPLE1). (For interpretation of the references to colour in this figure legend, the reader is referred to the Web version of this article.)

which verify the presence of some DNA point mutations. However, that model was from vestibular origin not peripheral, and it did not fully represent a paradigm of peripheral schwannoma in the context of SWN, thus other *in vitro* models resembling the pathology were needed. We developed and genetically characterized an immortalized schwannoma cell line, first trying to confirm the predicted cell growth capacity *in vitro*, and exploiting that it was correlated to the parent tumour *in vivo*. As expected in schwannomas, the DNA sequencing of these cells showed the presence of two pathogenic variants, affecting one allele of *NF2* and *LZTR1*, respectively. Bioinformatic analysis suggested the presence of a large deletion of the long arm of chromosome 22 encompassing *NF2* and *LZTR1* that was confirmed by cytogenetics tests. This finding is in agreement with the 4-hits/3-step mechanism required for schwannoma development, which involves inactivation of *NF2* and *SMARCB1* and/or *LTZR1* that are usually associated with pain [12,16], as exhibited by the patient. Although the unavailability of a patient's unaffected tissue did not allow to verify the germline origin of such

variants, we argue that as far as conceivable, the *LTZR1* mutation found would be in the germline, while the *NF2* mutation is somatic. In fact, unlike the *NF2* variant that is extremely rare, the *LZTR1* variant detected in SWN cells is present in the gnomAD population database with an allele frequency of 0.006 %, in agreement with the well-known reduced penetrance of LZTR1-related SWN.

Data on chromosome analyses on SCs are very limited in the literature. In HEI193 cells derived from a schwannoma obtained from a neurofibromatosis type 2 patient [28], we detected a hypotetraploid karyotype (data not shown), which is frequently observed after immortalization. In our cellular model, we performed chromosome analysis after XII passages in culture and found, beyond the molecular features characteristic of schwannomas with monoallelic variations in *LZTR1* and *NF2*, two different populations: one with monosomy of chromosome 22 and another showing hypotetraploid karyotype that maintained two copies of chromosome 22. Apart HEI193, however, other schwannoma cell lines from neurofibromatosis patients have been established [29], although they do not present all typical features of SWN-related tumours. Differently from our model, it must be highlighted that HEI193 are from vestibular and not from a peripheral schwannoma [28]. Although up to 95 % of vestibular schwannoma are sporadic and unilateral, others are bilateral and NF2-related SWN, ascribable to an *NF2* gene inactivation and subsequent loss of merlin function [30]. Unfortunately, HEI193 cells *in vitro* did not show the same growth pattern [31] as the hSCs from a SWN patient, which are here obtained. Li et al. [29], instead, isolated and immortalized hSCs from a neurofibromatosis type 1 patient. Even assuming that the terms "schwannoma" and neurofibroma" have been mingled for long times, until the recent re-classification [2], the hSCs from *NF1* neurofibromatosis patient are associated to a biallelic loss of *NF1* gene function and neurofibromin protein. This cell model, therefore, is clinically, genetically and biologically distinct for our hSCs from a *NF2/LTZR1* SWN patient.

Our analyses show that the schwannoma-derived cell line, here obtained, maintains the biological and phenotypic characteristics in terms of morphology and SCs markers, concomitant with the genetic traits and the tumorigenic potential of schwannomatosis. Namely, we repeatedly showed that the SCs markers, such S100, P0 and PMP22 proteins are retained through all the cell passages analysed, further confirming the quality of the SCs identity. The expression of these markers is a peculiar feature of SCs, also *in vitro*, covering all potential stages of their physiological differentiation [32].

Three hSC lines from schwannomatosis patients have already been reported by two different research groups [33,34]. Ostrow et al. [33] obtained two cell lines by SV40 virus immortalization from separate patients, clinically distinct as painful or not painful, respectively; however, the study seemed solely focused on schwannomas from the painful patient. In accordance with our approach, Ostrow et al. [33] found that SV40 did not alters the phenotype and biological characteristics of the hSC lines obtained. It is important to emphasize that the peculiarity of our results lies in the purification method, which ensures the SCs enrichment, and in the distinctive mutations found in the *LZTR1* and the *NF2* genes, the latter having never been reported so far. In parallel, also the cell line obtained by Allaf et al. [34], which were from a para-spinal and not form a peripheral tumor did not present either the *LTZR1* mutation or the *NF2* deletion that we found in our model.

In conclusion, we generated the first immortalized LTZR1-SWN cell line that retain essential genotype, phenotype, and cell growth patterns. These cells will be a valuable tool to advance research in SWN, and for prospective studies on the biomolecular aspects, as well as on the cellular and signalling pathways underlying the outset of schwannomas. Hopefully, the immortalization of that schwannoma type would also help to understand in more detail the pathogenesis of the less common LZTR1-related SWN.

Data availability statement

All data obtained and analysed in the study are included and available in the article and its supplementary materials.

Ethics statementstatement

All procedures were approved by the Ethical Committee of UNIMI (PRIN-2017BJJ5EE; Ethical Approval 95/2020) and meet the "Human participant declaration form" proposed by Heliyon. Material was obtained following written informed consent of patient from the Hospital "Santa Maria della Misericordia" (Rovigo, Italy); thereby, all contents presented in this study and associated data were deidentified and anonymized.

CRediT authorship contribution statement

Valentina Melfi: Methodology, Formal analysis. **Tasnim Mohamed:** Methodology, Investigation, Formal analysis. **Alessandra Colciago:** Supervision, Formal analysis, Data curation, Conceptualization. **Alessandra Fasciani:** Resources, Methodology. **Raffaele De Francesco:** Resources, Methodology. **Daniela Bettio:** Methodology, Investigation. **Cristina Cerqua:** Methodology, Investigation. **Francesca Boaretto:** Investigation, Formal analysis. **Elisabetta Basso:** Resources. **Stefano Ferraresi:** Resources. **Marco Montini:** Resources, Methodology. **Marica Eoli:** Resources. **Laura Papi:** Validation, Investigation, Funding acquisition. **Eva Trevisson:** Writing – original draft, Supervision, Funding acquisition, Data curation. **Valerio Magnaghi:** Writing – original draft, Validation, Supervision, Project administration, Funding acquisition, Conceptualization.

Declaration of competing interest

The authors declare the following financial interests/personal relationships which may be considered as potential competing interests: Valerio Magnaghi reports financial support was provided by the Ministry of University and Research (MUR). Other authors declare that they have no known competing financial interests or personal relationships that could have appeared to influence the work

reported in this paper.

Acknowledgments

The work was founded by Progetto di Eccellenza 2023–2027 and by PRIN 2017BJJ5EE, all from the Ministry of University and Research (MUR). The authors thank Dr. Veronica Bonalume, University of Milan, for investigation, data collection and technical assistance.

Appendix A. Supplementary data

Supplementary data to this article can be found online at https://doi.org/10.1016/j.heliyon.2024.e38957.

References

[1] N.A. Koontz, A.L. Wiens, A. Agarwal, C.M. Hingtgen, R.E. Emerson, K.M. Mosier, Schwannomatosis: the overlooked neurofibromatosis? AJR Am. J. Roentgenol. 200 (6) (2013) W646–W653.
[2] S.R. Plotkin, L. Messiaen, E. Legius, P. Pancza, R.A. Avery, J.O. Blakeley, D. Babovic- Vuksanovic, R. Ferner, M.J. Fisher, J.M. Friedman, M. Giovannini, D. H. Gutmann, C.O. Hanemann, M. Kalamarides, H. Kehrer-Sawatzki, B.R. Korf, V.F. Mautner, M. MacCollin, L. Papi, K.A. Rauen, V. Riccardi, E. Schorry, M. J. Smith, A. Stemmer-Rachamimov, D.A. Stevenson, N.J. Ullrich, D. Viskochil, K. Wimmer, K. Yohay, C. International Consensus Group on Neurofibromatosis Diagnostic, S.M. Huson, P. Wolkenstein, D.G. Evans, Updated diagnostic criteria and nomenclature for neurofibromatosis type 2 and schwannomatosis: an international consensus recommendation, Genet. Med. 24 (9) (2022) 1967–1977.
[3] K.W. Gripp, L. Baker, V. Kandula, J. Piatt, A. Walter, Z. Chen, L. Messiaen, Constitutional LZTR1 mutation presenting with a unilateral vestibular schwannoma in a teenager, Clin. Genet. 92 (5) (2017) 540–543.
[4] M.J. Smith, N.L. Bowers, M. Bulman, C. Gokhale, A.J. Wallace, A.T. King, S.K. Lloyd, S.A. Rutherford, C.L. Hammerbeck-Ward, S.R. Freeman, D.G. Evans, Revisiting neurofibromatosis type 2 diagnostic criteria to exclude LZTR1-related schwannomatosis, Neurology 88 (1) (2017) 87–92.
[5] D.G. Evans, N.L. Bowers, S. Tobi, C. Hartley, A.J. Wallace, A.T. King, S.K.W. Lloyd, S.A. Rutherford, C. Hammerbeck-Ward, O.N. Pathmanaban, S.R. Freeman, J. Ealing, M. Kellett, R. Laitt, O. Thomas, D. Halliday, R. Ferner, A. Taylor, C. Duff, E.F. Harkness, M.J. Smith, Schwannomatosis: a genetic and epidemiological study, J. Neurol. Neurosurg. Psychiatry 89 (11) (2018) 1215–1219.
[6] F. Rongioletti, F. Drago, A. Rebora, Multiple cutaneous plexiform schwannomas with tumors of the central nervous system, Arch. Dermatol. 125 (3) (1989) 431–432.
[7] S. Ogihara, A. Seichi, M. Iwasaki, H. Kawaguchi, T. Kitagawa, Y. Tajiri, K. Nakamura, Concurrent spinal schwannomas and meningiomas. Case illustration, J. Neurosurg. 98 (3 Suppl) (2003) 300.
[8] C. Bacci, R. Sestini, A. Provenzano, I. Paganini, I. Mancini, B. Porfirio, R. Vivarelli, M. Genuardi, L. Papi, Schwannomatosis associated with multiple meningiomas due to a familial SMARCB1 mutation, Neurogenetics 11 (1) (2010) 73–80.
[9] I. Christiaans, S.B. Kenter, H.C. Brink, T.A. van Os, F. Baas, P. van den Munckhof, A.M. Kidd, T.J. Hulsebos, Germline SMARCB1 mutation and somatic NF2 mutations in familial multiple meningiomas, J. Med. Genet. 48 (2) (2011) 93–97.
[10] S.R. Plotkin, J.O. Blakeley, D.G. Evans, C.O. Hanemann, T.J. Hulsebos, K. Hunter- Schaedle, G.V. Kalpana, B. Korf, L. Messiaen, L. Papi, N. Ratner, L.S. Sherman, M.J. Smith, A.O. Stemmer-Rachamimov, J. Vitte, M. Giovannini, Update from the 2011 international schwannomatosis workshop: from genetics to diagnostic criteria, Am. J. Med. Genet. 161A (3) (2013) 405–416.
[11] T.J. Hulsebos, A.S. Plomp, R.A. Wolterman, E.C. Robanus-Maandag, F. Baas, P. Wesseling, Germline mutation of INI1/SMARCB1 in familial schwannomatosis, Am. J. Hum. Genet. 80 (4) (2007) 805–810.
[12] I. Paganini, V.Y. Chang, G.L. Capone, J. Vitte, M. Benelli, L. Barbetti, R. Sestini, E. Trevisson, T.J. Hulsebos, M. Giovannini, S.F. Nelson, L. Papi, Expanding the mutational spectrum of LZTR1 in schwannomatosis, Eur. J. Hum. Genet. 23 (7) (2015) 963–968.
[13] A. Piotrowski, J. Xie, Y.F. Liu, A.B. Poplawski, A.R. Gomes, P. Madanecki, C. Fu, M.R. Crowley, D.K. Crossman, L. Armstrong, D. Babovic-Vuksanovic, A. Bergner, J.O. Blakeley, A.L. Blumenthal, M.S. Daniels, H. Feit, K. Gardner, S. Hurst, C. Kobelka, C. Lee, R. Nagy, K.A. Rauen, J.M. Slopis, P. Suwannarat, J. A. Westman, A. Zanko, B.R. Korf, L.M. Messiaen, Germline loss-of-function mutations in LZTR1 predispose to an inherited disorder of multiple schwannomas, Nat. Genet. 46 (2) (2014) 182–187.
[14] L. Tang, E. Nogales, C. Ciferri, Structure and function of SWI/SNF chromatin remodeling complexes and mechanistic implications for transcription, Prog. Biophys. Mol. Biol. 102 (2–3) (2010) 122–128.
[15] H. Kehrer-Sawatzki, S. Farschtschi, V.F. Mautner, D.N. Cooper, The molecular pathogenesis of schwannomatosis, a paradigm for the co-involvement of multiple tumour suppressor genes in tumorigenesis, Hum. Genet. 136 (2) (2017) 129–148.
[16] R. Sestini, C. Bacci, A. Provenzano, M. Genuardi, L. Papi, Evidence of a four-hit mechanism involving SMARCB1 and NF2 in schwannomatosis-associated schwannomas, Hum. Mutat. 29 (2) (2008) 227–231.
[17] S. Richards, N. Aziz, S. Bale, D. Bick, S. Das, J. Gastier-Foster, W.W. Grody, M. Hegde, E. Lyon, E. Spector, K. Voelkerding, H.L. Rehm, A.L.Q.A. Committee, Standards and guidelines for the interpretation of sequence variants: a joint consensus recommendation of the American college of medical genetics and genomics and the association for molecular pathology, Genet. Med. 17 (5) (2015) 405–424.
[18] An International System for Human Cytogenomic Nomenclature, 2020. S.Karger AG2020.
[19] U. Hanses, M. Kleinsorge, L. Roos, G. Yigit, Y. Li, B. Barbarics, I. El-Battrawy, H. Lan, M. Tiburcy, R. Hindmarsh, C. Lenz, G. Salinas, S. Diecke, C. Muller, I. Adham, J. Altmuller, P. Nurnberg, T. Paul, W.H. Zimmermann, G. Hasenfuss, B. Wollnik, L. Cyganek, Intronic CRISPR repair in a preclinical model of noonan syndrome-associated cardiomyopathy, Circulation 142 (11) (2020) 1059–1076.
[20] F. Deng, D.G. Evans, M.J. Smith, Comparison of the frequency of loss-of-function LZTR1 variants between schwannomatosis patients and the general population, Hum. Mutat. 43 (7) (2022) 919–927.
[21] M.J. Smith, B. Isidor, C. Beetz, S.G. Williams, S.S. Bhaskar, W. Richer, J. O'Sullivan, B. Anderson, S.B. Daly, J.E. Urquhart, A. Fryer, C.F. Rustad, S.J. Mills, A. Samii, D. du Plessis, D. Halliday, S. Barbarot, F. Bourdeaut, W.G. Newman, D.G. Evans, Mutations in LZTR1 add to the complex heterogeneity of schwannomatosis, Neurology 84 (2) (2015) 141–147.
[22] H.S. Schwartz, G.A. Allen, M.G. Butler, Telomeric associations, Appl Cytogenet 16 (6) (1990) 133–137.
[23] K.T. Tan, M.K. Slevin, M.L. Leibowitz, M. Garrity-Janger, H. Li, M. Meyerson, Neotelomeres and telomere-spanning chromosomal arm fusions in cancer genomes revealed by long-read sequencing, bioRxiv (2023).
[24] C. Forde, M.J. Smith, G.J. Burghel, N. Bowers, N. Roberts, T. Lavin, J. Halliday, A.T. King, S. Rutherford, O.N. Pathmanaban, S. Lloyd, S. Freeman, D. Halliday, A. Parry, P. Axon, J. Buttimore, S. Afridi, R. Obholzer, R. Laitt, O. Thomas, S.M. Stivaros, G. Vassallo, D.G. Evans, NF2-related schwannomatosis and other schwannomatosis: an updated genetic and epidemiological study, J. Med. Genet. (2024).

[25] A. Cuevas-Navarro, L. Rodriguez-Munoz, J. Grego-Bessa, A. Cheng, K.A. Rauen, A. Urisman, F. McCormick, G. Jimenez, P. Castel, Cross-species analysis of LZTR1 loss-of- function mutants demonstrates dependency to RIT1 orthologs, Elife 11 (2022).
[26] J. Vitte, F. Gao, G. Coppola, A.R. Judkins, M. Giovannini, Timing of Smarcb1 and Nf2 inactivation determines schwannoma versus rhabdoid tumor development, Nat. Commun. 8 (1) (2017) 300.
[27] G. Hung, R. Faudoa, X. Li, Z. Xeu, D.E. Brackmann, W. Hitselberg, E. Saleh, F. Lee, D.H. Gutmann, W. Slattery 3rd, J.S. Rhim, D. Lim, Establishment of primary vestibular schwannoma cultures from neurofibromatosis type-2 patients, Int. J. Oncol. 14 (3) (1999) 409–415.
[28] G. Hung, X. Li, R. Faudoa, Z. Xeu, L. Kluwe, J.S. Rhim, W. Slattery, D. Lim, Establishment and characterization of a schwannoma cell line from a patient with neurofibromatosis 2, Int. J. Oncol. 20 (3) (2002) 475–482.
[29] H. Li, L.J. Chang, D.R. Neubauer, D.F. Muir, M.R. Wallace, Immortalization of human normal and NF1 neurofibroma Schwann cells, Lab. Invest. 96 (10) (2016) 1105–1115.
[30] N. Pecina-Slaus, Merlin, the NF2 gene product, Pathol. Oncol. Res. 19 (3) (2013) 365–373.
[31] O. Saydam, G.B. Ozdener, O. Senol, A. Mizrak, S. Prabhakar, A.O. Stemmer- Rachamimov, X.O. Breakefield, G.J. Brenner, A novel imaging-compatible sciatic nerve schwannoma model, J. Neurosci. Methods 195 (1) (2011) 75–77.
[32] R. Mirsky, A. Woodhoo, D.B. Parkinson, P. Arthur-Farraj, A. Bhaskaran, K.R. Jessen, Novel signals controlling embryonic Schwann cell development, myelination and dedifferentiation, J. Peripher. Nerv. Syst. 13 (2) (2008) 122–135.
[33] K.L. Ostrow, K. Donaldson, J. Blakeley, A. Belzberg, A. Hoke, Immortalized human Schwann cell lines derived from tumors of schwannomatosis patients, PLoS One 10 (12) (2015) e0144620.
[34] A. Allaf, B. Victoria, R. Rosario, C. Misztal, S. Humayun Gultekin, C.T. Dinh, C. Fernandez- Valle, WP1066 induces cell death in a schwannomatosis patient-derived schwannoma cell line, Cold Spring Harb Mol Case Stud 8 (4) (2022).